CODEN STJSAO
ZX470/1367

ISSN 0562-1887
UDK 658.511/.512:65.012.11:004.421

Numerical Procedure for Two Beam Elastic Impact Analysis

***Ivan ĆATIPOVIĆ*[1)], *Nikola VLADIMIR*[1)] and *Marin RELJIĆ*[2)]**

1) Fakultet strojarstva i brodogradnje Sveučilišta u Zagrebu (Faculty of Mechanical Engineering and Naval Architecture, University of Zagreb) Ivana Lučića 5, HR - 10000 Zagreb **Republic of Croatia**

2) Brodarski Institut d.o.o. Av. V. Holjevca 20, HR - 10020 Zagreb **Republic of Croatia**

ivan.catipovic@fsb.hr

Keywords
Elastic impact
Energy method
FEM
Linear acceleration method

Ključne riječi
Elastični sudar
Energijska metoda
MKE
Metoda linearnog ubrzanja

Received (primljeno): 2008-02-20
Accepted (prihvaćeno): 2008-12-19

Original scientific paper

The procedure for numerical analysis of the elastic impact of two beams is presented. The beams are modelled by using the FEM technique, and for time integration of dynamic equilibrium equation the modified linear acceleration method is applied. Special attention is paid to contact problem and to calculation execution. A short review of the energy conservation principle based method for impact force determination is also given. The procedure is illustrated with the case of collision of communication bridge between two offshore platforms and the protective construction, called arrestor. The results are compared to those obtained by energy conservation principle based method. The study of damping influence on system dynamic response is also added.

Numerički postupak za analizu elastičnog sudara dviju greda

Izvornoznanstveni članak

Prikazan je postupak za numeričku analizu elastičnog sudara dviju greda. Grede su modelirane korištenjem metode konačnih elemenata, a za vremensku integraciju jednadžbe dinamičke ravnoteže korištena je modificirana metoda linearnog ubrzanja. Posebna pozornost posvećena je kontaktnom problemu i provedbi proračuna. Ukratko je opisana metoda za određivanje sile udara temeljena na principu očuvanja energije. Primjena postupka ilustrirana je na primjeru sudara komunikacijskog mosta između dviju platformi i zaštitne konstrukcije, zvane "arestor". Dobiveni rezultati uspoređeni su s rezultatima određenim energetskim pristupom. Analiziran je i utjecaj prigušenja na dinamički odziv sustava.

1. Introduction

The procedure for numerical analysis of the elastic impact of two beams, based on linear acceleration method, is presented. Motivation for this work is found in the practical engineering problem of analysing impact response of the communication bridge between two offshore platforms and protective construction called arrestor. It is common to find two offshore facilities at one oil and gas exploitation place. The first of them, which is usually fixed, is used to maintain all technology operations needed for oil and gas exploitation. The second one is used for crew accommodation. Efficient connection of these facilities is achieved through a communication bridge for crew and material transport, Figure 1. The bridge interconnects fixed and floating facilities. Thus, one support is fixed and another one is movable. When facilities mentioned are distant there is the possibility of the bridge pitching into the sea. So, the task of the arrestor is to restrain the bridge without plastic deformation. There are many types of arrestors and also a few calculation procedures available, for example procedures based on energy conservation principle [1], and some procedures which assume the plastic deformation of the arrestor. The authors prefer elastic calculation methodology, although it is rarely used, because when the arrestor is designed in that way, it can be used in similar situations.

2. Numerical procedure

Two elastic beams, i.e. upper and lower beam, are under consideration, Figure 2. One end of the upper beam is sliding supported, and the other one is hinge jointed. If sliding support is moved off, the upper beam is pitching and strikes the free end of the second beam. Another end of the lower beam is fixed. This is the start of dynamic interaction of beams, i.e. alteration of contact and non-contact stages. The basic equation of dynamic equilibrium yields [2]:

Symbols/Oznake

A_c - cross-section area of contact element
- površina presjeka kontaktnog elementa

d - horizontal distance between lower beam support and end
- horizontalna udaljenost između oslonca i kraja donje grede

E - Young's modulus
- Youngov modul elastičnosti

$E_{def,\,a}$ - arrestor strain energy
- energija deformacije arestora

$E_{def,\,b}$ - bridge strain energy
- energija deformacije mosta

F_c - contact element load
- opterećenje kontaktnog elementa

F_{din} - dynamic contact force
- dinamička kontaktna sila

g - acceleration of gravity
- gravitacijsko ubrzanje

h - vertical distance between the upper beam centre of gravity at initial and instant at impact time,
- vertikalna udaljenost između težišta gornje grede u početnom trenutku i trenutku udara

h_{din} - vertical distance between the upper beam centre of gravity at instant impact time and at instant maximum deflection instant
- vertikalna udaljenost između težišta gornje grede u trenutku udara i maksimalnog progiba

i - time step, s
- vremenski korak

J_u - upper beam mass inertia moment
- moment tromosti mase gornje grede

K_f - flexion coefficient
- koeficijent fleksije

l_c - contact element length
- duljina kontaktnog elementa

l_l - lower beam length
- duljina donje grede

l_u - upper beam length
- duljina gornje grede

M_b - bridge bending moment
- moment savijanja mosta

$M_{G,\,u}$ - upper beam weight moment
- moment težine gornje grede

m_i - modal mass for certain vibration mode
- modalna masa za određeni oblik vibriranja

m_l - lower beam mass
- masa donje grede

m_u - upper beam mass
- masa gornje grede

q_l - lower beam distributed load
- distribuirano opterećenje donje grede

q_u - upper beam distributed load
- distribuirano opterećenje gornje grede

t - time variable
- vrijeme

t_0 - time when upper beam is in horizontal position
- trenutak kada je gornja greda u horizontalnom položaju

w_{din} - dynamic deflection
- dinamički progib

$y_{k,\,l}$ - degree of freedom of lower beam where there is contact
- stupanj slobode donje grede na mjestu kontakta

$y_{k,\,u}$ - degree of freedom of upper beam where contact is realized
- stupanj slobode gornje grede na mjestu kontakta

$[\mathbf{C}]$ - damping matrix
- matrica prigušenja

$[\mathbf{C}_l]$ - lower beam global damping matrix
- globalna matrica prigušenja donje grede

$[\mathbf{C}_u]$ - upper beam global damping matrix
- globalna matrica prigušenja gornje grede

$[\mathbf{K}]$ - stiffness matrix
- matrica krutosti

$[\mathbf{K}_c]$ - contact element stiffness matrix
- matrica krutosti kontaktnog elementa

$[\mathbf{K}_l]$ - lower beam global stiffness matrix
- globalna matrica krutosti donje grede

$[\mathbf{K}_u]$ - upper beam global stiffness matrix
- globalna matrica krutosti gornje grede

$[\mathbf{M}]$ - mass matrix
- matrica mase

$[\mathbf{M}_l]$ - lower beam global mass matrix
- globalna matrica masa donje grede

$[\mathbf{M}_u]$ - upper beam global mass matrix
- globalna matrica masa gornje grede

$[\mathbf{P}]$, $[\mathbf{Q}]$, $[\mathbf{R}]$ - auxiliary matrices
- pomoćne matrice

[**S**] - auxiliary matrices
- pomoćne matrice

[**Φ**] - natural vibration modes matrix
- matrica prirodnih oblika vibriranja

$\{F(t)\}$ - force vector
- vektor sile

$\{F_l\}$ - lower beam nodal forces vector
- vektor čvornih sila donje grede

$\{F_u\}$ - upper beam nodal forces vector
- vektor čvornih sila gornje grede

$\{f\}_{i+1}$ - auxiliary vector
- pomoćni vektor

$\{\delta\}$ - displacement vector
- vektor pomaka

$\{\delta_l\}$ - lower beam displacement vector
- vektor pomaka donje grede

$\{\delta_u\}$ - upper beam displacement vector
- vektor pomaka gornje grede

$\{\dot{\delta}\}$ - velocity vector
- vektor brzine

$\{\dot{\delta}_l\}$ - lower beam velocity vector
- vektor brzine donje grede

$\{\dot{\delta}_u\}$ - upper beam velocity vector
- vektor brzine gornje grede

$\{\ddot{\delta}\}$ - acceleration vector
- vektor ubrzanja

$\{\ddot{\delta}_l\}$ - lower beam acceleration vector
- vektor ubrzanja donje grede

$\{\ddot{\delta}_u\}$ - upper beam acceleration vector
- vektor ubrzanja gornje grede

α_u - upper beam inclining angle
- kut nagiba gornje grede

α_{u0} - upper beam initial inclining angle
- početni nagib gornje grede

γ_i - non-dimensional damping coefficient for certain vibration mode
- bezdimenzijski koeficijent prigušenja za određeni oblik vibriranja

Δt - interval duration
- vremenski interval

ε_u - upper beam angular acceleration
- kutno ubrzanje gornje grede

ω_i - natural frequency of certain vibration mode
- prirodna frekvencija određenog oblika vibriranja

ω_u - upper beam angular velocity
- kutna brzina gornje grede

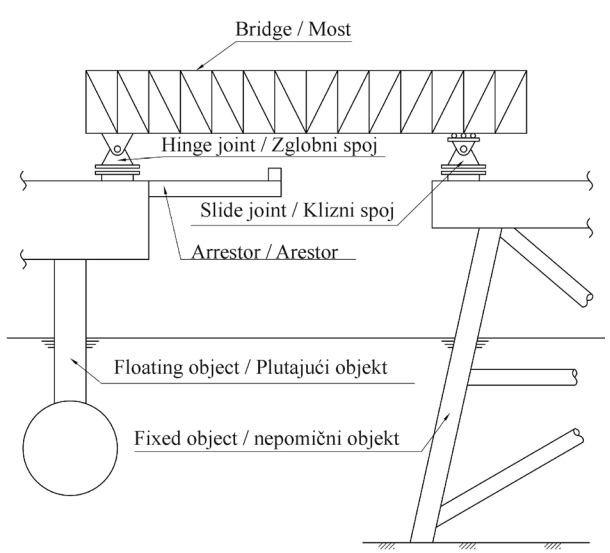

Figure 1. Schematic view of bridge and arrestor
Slika 1. Shematski prikaz mosta i arestora

$$[K]\{\delta\} + [C]\{\dot{\delta}\} + [M]\{\ddot{\delta}\} = \{F(t)\} \quad (1)$$

Global stiffness and mass matrices for upper and lower beam are defined according to [2], and global damping matrices for upper and lower beam are defined according to [3]. Two types of finite elements are used; beam 4DOF finite element and bar 2DOF finite element. Beam elements are used for the upper and lower beam and the bar element is used for impact location modeling (contact element). The role of the contact element is the description of local behavior of both beams near the impact place. Since the procedure intends to give a global response, the influence of considered contact element on global deformations of the rest of the construction should be minimized. It is achieved by a relatively large stiffness of contact element. This way, only the elastic deformation of contact element is allowed.

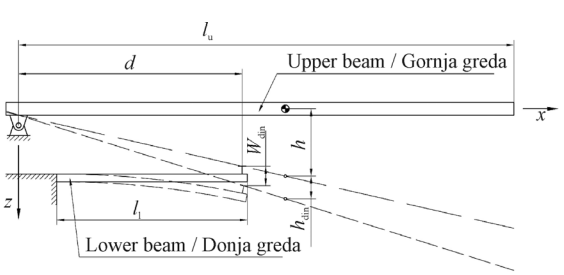

Figure 2. Disposition of upper and lower beam
Slika 2. Dispozicija gornje i donje grede

During the pitching of the upper one, the considered beams are two independent bodies. Only during the contact can these beams be treated as one structure. It is also obvious that the beams are not in contact from instant impact time till instant resting time. Moreover, the interaction of considered beams consists of a number of contact and non-contact periods. In other words, we can say that the contact of beams can sustain only compressive but not a tensile force. This fact should be taken into account when defining the system of motion equations. Therefore, by means of Eq. (1) two systems with two possible stages of beams interaction should be defined, i.e. the first one without the contact and the second one with contact. The first stage, where two independent bodies are inherent, is defined by:

$$\begin{bmatrix}[K_\mathrm{l}] & [0]\\ [0] & [K_\mathrm{u}]\end{bmatrix}\begin{Bmatrix}\{\delta_\mathrm{l}\}\\ \{\delta_\mathrm{u}\}\end{Bmatrix}+\begin{bmatrix}[C_\mathrm{l}] & [0]\\ [0] & [C_\mathrm{u}]\end{bmatrix}\begin{Bmatrix}\{\dot\delta_\mathrm{l}\}\\ \{\dot\delta_\mathrm{u}\}\end{Bmatrix}+$$
$$+\begin{bmatrix}[M_\mathrm{l}] & [0]\\ [0] & [M_\mathrm{u}]\end{bmatrix}\begin{Bmatrix}\{\ddot\delta_\mathrm{l}\}\\ \{\ddot\delta_\mathrm{u}\}\end{Bmatrix}=\begin{Bmatrix}\{F_\mathrm{l}\}\\ \{F_\mathrm{u}\}\end{Bmatrix}. \tag{2}$$

During contact, both beams behave as a unique structure, so the coupling should be introduced into a system of equation (2). The coupling is achieved through new stiffness matrix, because inertial and damping forces take effect on both beams independently. The new global stiffness matrix is made by imposing the bar 2DOF finite element stiffness matrix into the old one. So, the following matrix [2]:

$$[K_\mathrm{c}]=\frac{EA_\mathrm{c}}{l_\mathrm{c}}\begin{bmatrix}1 & -1\\ -1 & 1\end{bmatrix}, \tag{3}$$

is added up together with matching terms in the old stiffness matrix. Now, the global stiffness matrix can be shown in the following form:

$$[K]=\begin{bmatrix}\cdots & y_{k,l} & \cdots & y_{k,u} & \cdots\\ \cdots & +\frac{EA_c}{l_c} & \cdots & -\frac{EA_c}{l_c} & \cdots\\ \cdots & -\frac{EA_c}{l_c} & \cdots & +\frac{EA_c}{l_c} & \cdots\end{bmatrix} \tag{4}$$

Since contact and non-contact stages alternate, the condition that indicates the starting and the ending of each stage is the appearance and disappearance of compressive load in contact element. So the condition yields:

$$F_\mathrm{c}=\frac{EA_\mathrm{c}}{l_\mathrm{c}}\left(y_{\mathrm{k,u}}-y_{\mathrm{k,l}}\right)<0. \tag{5}$$

It is more suitable to replace Eq. (5) with the following one:

$$y_{\mathrm{k,u}}-y_{\mathrm{k,l}}<0. \tag{6}$$

Thus, if the condition in Eq. (6) is satisfied, there is contact between the beams. Otherwise the beams are in a non-contact stage.

2.1. Linear acceleration method

Numerical integration of Eq. (1) is done by using the linear acceleration method [3]. This method assumes linear acceleration in specified time interval. Acceleration vector is determined according to:

$$\{\ddot\delta\}_{i+1}=[S]^{-1}\{f\}_{i+1}, \tag{7}$$

where:

$$\{f\}_{i+1}=\{F(t)\}_{i+1}-\left([P]\{\delta\}_i+[Q]\{\dot\delta\}_i+[R]\{\ddot\delta\}_i\right). \tag{8}$$

Integration matrix is defined by the following formula:

$$[S]=[M]+\frac{\Delta t}{2}[C]+\frac{\Delta t^2}{6}[K]. \tag{9}$$

Auxiliary matrices are defined in the following form:

$$\begin{aligned}&[P]=[K],\\ &[Q]=[C]+\Delta t[K],\\ &[R]=\frac{\Delta t}{2}[C]+\frac{\Delta t^2}{3}[K].\end{aligned} \tag{10}$$

Velocity and displacement vector at time instant t_{i+1}

$$\begin{aligned}&\{\dot\delta\}_{i+1}=\{\dot\delta\}_i+\frac{1}{2}\Delta t\left(\{\dot\delta\}_i+\{\ddot\delta\}_{i+1}\right),\\ &\{\delta\}_{i+1}=\{\delta\}_i+\Delta t\{\dot\delta\}_i+\frac{\Delta t^2}{3}\{\ddot\delta\}_i+\frac{\Delta t^2}{6}\{\ddot\delta\}_{i+1}.\end{aligned} \tag{11}$$

The linear acceleration method shown here slightly differs from that given in [3]. Although there the displacement is calculated first, here it is necessary to first calculate the acceleration and then the velocity and displacement. Otherwise, numerical instability can occur when very low interval duration Δt is used, because of subtraction of very close numbers. When the linear acceleration method is used in recommended form, it is numerically stable.

2.2. Load

It is assumed that the external load is caused only by gravitational force. Taking into account that cross-

section of beams is assumed to be uniform, the weight is uniformly distributed per length. Distributed load of upper beam:

$$q_{\mathrm{u}}(x)=\frac{m_{\mathrm{u}}g}{l_{\mathrm{u}}} \tag{12}$$

and for distributed load of the lower beam:

$$q_l(x)=\frac{m_l g}{l_l}. \tag{13}$$

2.3. Initial conditions

It is assumed that in instant initial time the lower beam is in a horizontal and the upper beam is in an inclined position. The initial inclination angle is α_{u0}. This topology is used because it is easy to satisfy the compatibility of beam deflections, but some other topology is also allowed. During pitching, the upper beam rotates around the joint as a rigid body. The equation of motion has the following form:

$$J_{\mathrm{u}}\,\varepsilon_{\mathrm{u}}+M_{\mathrm{G,u}}=0. \tag{14}$$

The beam mass moment of inertia is calculated by:

$$J_{\mathrm{u}}=\frac{1}{3}m_{\mathrm{u}}l_{\mathrm{u}}^2 \tag{15}$$

and the upper beam weight moment by:

$$M_{\mathrm{G,u}}=-\frac{1}{2}m_{\mathrm{u}}\,g\,l_{\mathrm{u}}. \tag{16}$$

By substituting (15) and (16) into (14) and after editing, the following expression is derived:

$$\varepsilon_{\mathrm{u}}=\frac{3}{2}\frac{g}{l_{\mathrm{u}}}. \tag{17}$$

By integrating Eq. (17) the upper beam angular velocity is derived:

$$\omega_{\mathrm{u}}=\frac{3}{2}\frac{g}{l_{\mathrm{u}}}t. \tag{18}$$

Integration of Eq. (18) gives the value of the upper beam inclining angle during pitching:

$$\alpha_{\mathrm{u}}=\frac{3}{4}\frac{g}{l_{\mathrm{u}}}t^2. \tag{19}$$

The initial inclination angle is calculated by using the following formula:

$$\alpha_{u0}=\tan\frac{h}{\frac{l_u}{2}}. \tag{20}$$

Then, the time when the upper beam is in horizontal position:

$$t_0=\sqrt{\frac{4}{3}\frac{l_u}{g}\tan\frac{h}{\frac{l_u}{2}}} \tag{21}$$

and taking Eq. (18) into account, the angular velocity in horizontal position:

$$\omega_{\mathrm{u0}}=\frac{3}{2}\frac{g}{l_{\mathrm{u}}}t_0. \tag{22}$$

Initial conditions for the upper beam $\{\dot{\delta}_{\mathrm{u}}\}_0$ and $\{\ddot{\delta}_{\mathrm{u}}\}_0$ are defined by using Eqs. (17), (20) and (22) and follow the next model:

	velocity	acceleration
deflection	$k_{\mathrm{i}}\omega_{\mathrm{u0}}$	$k_{\mathrm{i}}\varepsilon_{\mathrm{u}}$
inclination angle	ω_{u0}	ε_{u}

(23)

where k_i is the horizontal distance from a certain node to an upper beam joint.

For satisfying the motion equation in the initial time instant, deflection is calculated by using the following formula:

$$\{\delta_{\mathrm{u}}\}_0=[K_{\mathrm{u}}]_0\left(\{F_{\mathrm{u}}\}_0-[C_{\mathrm{u}}]\{\dot{\delta}_{\mathrm{u}}\}_0-[M_{\mathrm{u}}]\{\ddot{\delta}_{\mathrm{u}}\}_0\right). \tag{24}$$

The initial velocity of the lower beam is zero so one can write:

$$\{\dot{\delta}_{\mathrm{l}}\}_0=\{0\};\quad \{\ddot{\delta}_{\mathrm{l}}\}_0=\{0\}. \tag{25}$$

Initial deflection:

$$\{\delta_{\mathrm{l}}\}_0=[K_{\mathrm{l}}]^{-1}\{F_{\mathrm{l}}\}_0, \tag{26}$$

where $\{F_l\}_0$ is the initial force vector of the lower beam.

3. Energy conservation principle approach

The impact force between to given beams can be calculated by applying the energy conservation principle. In the instant initial time instant the upper beam has a gravitational potential energy which is transformed into kinetic energy during the fall. After the impact, kinetic energy of the upper beam transforms into kinetic energy of the lower beam and the strain energy of the upper and the lower beam. The energy dissipation during impact, like friction or damping dissipation or plastic deformations near the impact location, are not taken into account. There are also two restrictions; it is assumed that the stiffness of the upper beam is several times higher than the lower beam stiffness, so the upper beam strain energy is negligible when compared to lower beam strain energy. We also assume that there is zero velocity at maximum deflection of the lower beam, so the kinetic energy of both beams equals zero. Taking into account

the previously mentioned simplification, we can presume that gravitation potential energy of the upper beam transforms into the strain energy of the lower beam [1]

$$m_u g\left(h+h_{din}\right)=\frac{1}{2}F_{din}w_{din}\,. \tag{27}$$

Bearing in mind Figure 2 one can write:

$$h_{din}=\frac{l_u}{2d}w_{din}\,. \tag{28}$$

Maximum of dynamic contact force is achieved when maximum w_{din}

$$F_{din}=k_f w_{din}\,. \tag{29}$$

By introducing Eqs. (28) and (29) into (27) one can write:

$$m_u g\left(h+\frac{l_u}{2d}w_{din}\right)=\frac{1}{2}k_f w_{din}\,, \tag{30}$$

$$\frac{1}{2}k_f w_{din}^2-\frac{m_u g l_u}{2d}w_{din}+m_u g h=0\,. \tag{31}$$

This quadratic equation gives the dynamic deflection of the lower beam end

$$w_{din}=\frac{m_u g l_u \pm\sqrt{m_u g(8d^2 h k_f+m_u g l_u^2)}}{2d k_f}\,. \tag{32}$$

Only the positive solution fits the physical background so one can write

$$w_{din}=\frac{m_u g l_u +\sqrt{m_u g(8d^2 h k_f+m_u g l_u^2)}}{2d k_f}\,. \tag{33}$$

4. Illustrative example

The collision of the communication bridge between two offshore platforms and the arrestor is analysed. It is assumed that in the initial instant the bridge is leaned on both ends, Figure 1. When the platforms are distant, the bridge starts to pitch and strikes the arrestor. The bridge is a braced construction, and is made of high-tensile steel, Figure 3. Properties of the bridge are the following [4]:

Mass	m_b = 12 t
Length	l_b = 29 m
Second moment of cross-section over	I_b = 0,01831 m^4
Section modulus	W_b = 0,009978 m^3
Young's modulus	E_b = 2,1×10^5 MPa
Maximum bending stress	$\sigma_{al,b}$ = 533 MPa

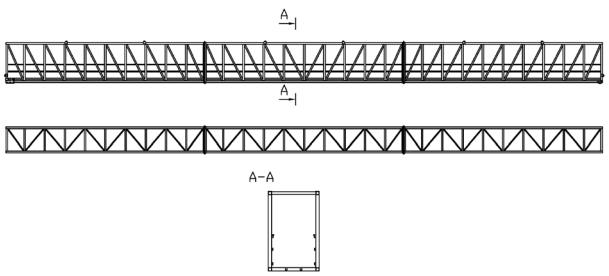

Figure 3. Bridge structure

Slika 3. Struktura mosta

The arrestor is a protective construction consisting of two longitudinal beams and one transverse beam, Figure 4. Geometrical properties of the arrestor I profile are the following:

Height	300	mm
Breadth	1000	mm
Web breadth	20	mm
Flange thickness	24	mm
Second moment of cross-section over	0,001038	m^4
Section modulus	0,006918	m^3
Cross-section area	0,05374	m^2
Shear area	0,006	m^2

Material properties of the arrestor:

Young's modulus	E_a	= 2,1x10^5	N/mm^2
Maximum bending stress	$\sigma_{al,a}$	= 533	N/mm^2
Maximum shear stress	$\tau_{al,a}$	= 355	N/mm^2

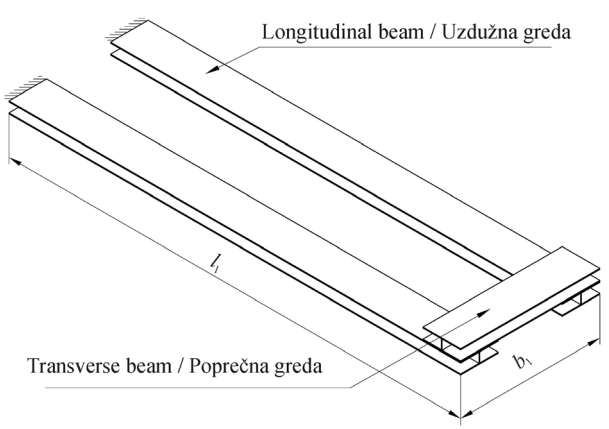

Figure 4. Arrestor structure

Slika 4. Arestor

It is obvious that both the bridge and the arrestor can be treated as uniform beams. Properties of the arrestor used in numerical calculation and treated as uniform beam are:

Mass	m_a = 11,7 t
Length	l_a = 12 m
Breadth	b_a = 3,7 m

Cross-section moment of inertia $I_a = 0{,}002075$ m^4

Section modulus $W_a = 0{,}01384$ m^3

Shear area $A_{s,a} = 0{,}012$ mm^2

Numerical analysis is done with 22 finite elements. The FEM topology is shown in Figure 5. Simulation duration is 3 s and 90 000 time steps are necessary. Time step duration in non-contact stage is 5×10^{-5} s and for contact stage $2{,}5\times10^{-5}$, respectively. Contact element length is chosen to be 0,3 m, and its cross-section area $A_c = 0{,}04$ m^2. Assessment of damping matrix for bridge and arrestor is based on critical damping value with given proportionality value. Global damping matrix is calculated by the following formula [3]:

$$[C] = [\Phi]^{-T} \lceil 2\gamma_i \omega_i m_i \rfloor [\Phi]^{-1}. \tag{34}$$

The non-dimensional damping coefficient value is taken to be $\gamma_i = 0{,}03$.

Arrestor end is on the position of node 8, and contact position on the bridge is presented by node 16. Deflection of these nodes is shown in Figure 6. Critical cross-section of the arrestor is at the clamp position, i.e. node 1, and the critical cross-section of the bridge is in the contact node, Figure 7. Shear stress of the arrestor at clamp position is presented in Figure 8 and the contact element stress is shown in Figure 9. Comparison of derived numerical results to those obtained by energy conservation approach is shown in Table 1.

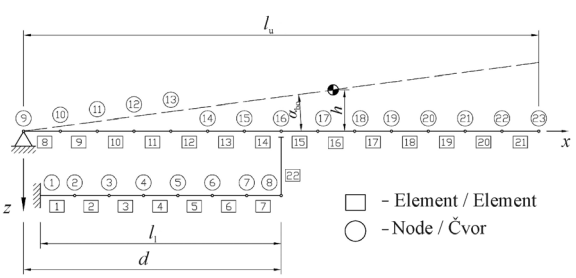

Figure 5. FEM topology of bridge and arrestor

Slika 5. Topologija konačnih elemenata mosta i arestora

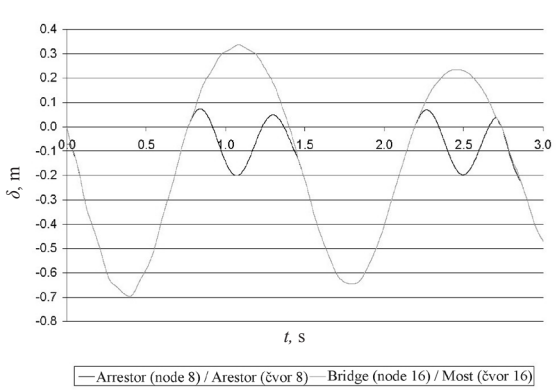

Figure 6. Deflection of arrestor end (node 8) and bridge at contact position (node 16)

Slika 6. Progib kraja arestora (čvor 8) i mosta na mjestu kontakta (čvor 16)

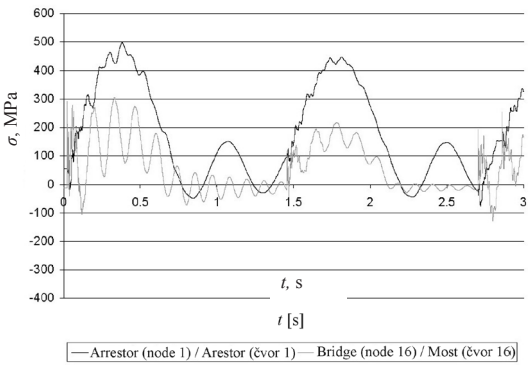

Figure 7. Bending stress at critical cross-sections of arrestor (node 1) and bridge (node 16)

Slika 7. Savojno naprezanje u kritičnim presjecima arestora (čvor 1) i mosta (čvor 16)

The assumption that the strain energy of the bridge is negligible when compared to the strain energy of the arrestor is also checked. The strain energy of the arrestor is calculated according to:

$$E_{def,a} = \frac{1}{2} F_{din} \cdot w_{din} \tag{35}$$

and equals $E_{def,a} = 149{,}2$ kJ.

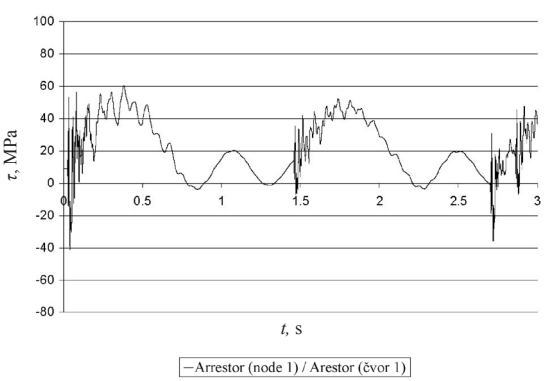

Figure 8. Shear stress of arrestor (node 1)

Slika 8. Smično naprezanje u arestoru (čvor 1)

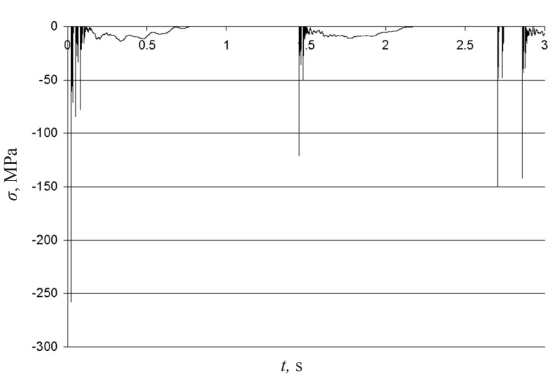

Figure 9. Contact element stress

Slika 9. Naprezanje u kontaktnom elementu

Table 1. Results comparison
Tablica 1. Usporedba rezultata

	(1) FEM / Metoda konačnih elemenata	(2) Energy approach / Energijski pristup	(1)/(2)
$w_{\text{din,a}}$	0,691 m	0,628 m	1,100
$\sigma_{\text{din,a}}$	492 MPa	412 MPa	1,194
$\tau_{\text{din,a}}$	59 MPa	40 MPa	1,475
$\sigma_{\text{din,b}}$	295 MPa	219 MPa	1,347

The strain energy of the bridge [1] is calculated by the following formula:

$$E_{\text{def,b}} = \frac{1}{2}\int_0^{l_m} \frac{M_{\text{b}}^2(x)}{E_{\text{b}} I_{\text{b}}}\,\mathrm{d}\,x \tag{36}$$

and when arrestor deflection is maximum, it equals $E_{\text{def,b}}$ = 4,4 kJ. It is obvious that the bridge strain energy makes only 3,0 % of the arrestor strain energy. It is also well known that in steel constructions vibrations analysis damping forces are negligible when compared to inertial and restoring forces. These constructions vibrate in phase, and when deflection is maximal the vibration velocity is relatively small.

The agreement of the results is acceptable in case of deflection and stresses of the arrestor. Large discrepancies are found in case of bending stress of the bridge. Bridge shear stress is not calculated since shear stress for braced construction is negligible. Calculation of natural frequencies and natural modes of uncoupled and coupled vibrations has been done. Natural modes are shown in Figures 10 to 12. Natural frequencies and natural modes are presented in Tables 2 and 3.

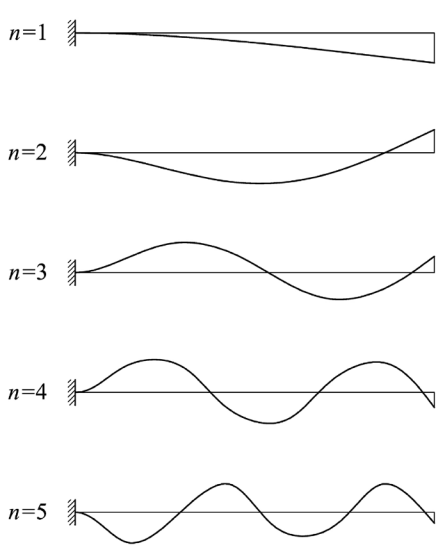

Figure 10. Natural modes of arrestor
Slika 10. Prirodni oblici vibriranja arestora

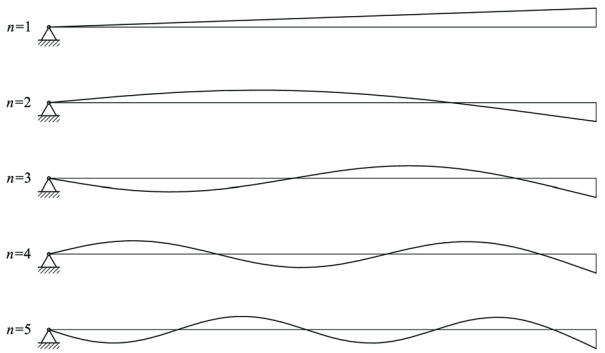

Figure 11. Natural modes of bridge
Slika 11. Prirodni oblici vibriranja mosta

It can be seen in Figure 6 that during the interaction of the bridge and the arrestor, from 0,77 s to 1,44 s, there is no contact. During that time the arrestor is vibrating freely, and from 0,77 s to 1,24 s makes one oscillation which takes 0,47 s. The duration of the mentioned oscillation is nearly a natural period of the arrestor for the first natural mode, Figure 10. Therefore, one can conclude that the arrestor is oscillating in first mode in non contact-stage. A similar conclusion can be derived from looking into Figures 7 and 8. Figure 7 shows that stress level varies with period 0,12 s to 0,14 s, irrespective of contact or non-contact stage. This period is close to the second natural period of the bridge, Figure 11, and the second natural mode of coupled vibrations of bridge and arrestor, Figure 12. One can conclude that in bridge vibrations the second natural mode is dominant.

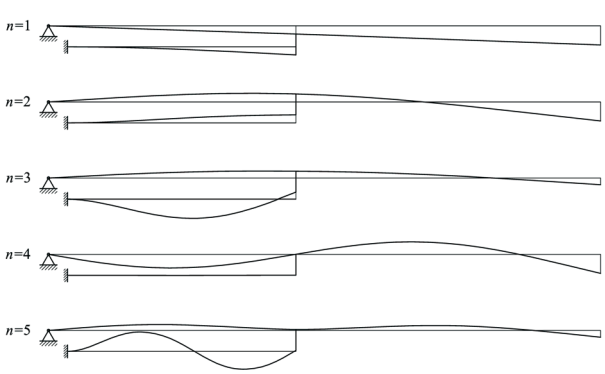

Figure 12. Natural modes of bridge and arrestor – coupled motion
Slika 12. Prirodni oblici spregnutih vibracija mosta i arestora

5. Conclusion

The presented numerical procedure for the analysis of the elastic impact of two beams seems to be more suitable for detailed structural analysis, since the energy approach principle is more convenient for standard engineering practice. The energy approach is especially

appropriate in design phase. Comparison of the results showed good agreement between deflections and stresses at critical arrestor cross-section, but large discrepancies occurred in stress calculation at critical cross-section of bridge. There are two reasons why this is the case. The first is that critical cross-section of the arrestor is rather distant from contact location, where large local stresses and deformations are present. Considering the bridge, the situation is opposite, since the critical cross-section is at contact location. It is well known that energy approach cannot capture local deformations and stresses, and therefore it gives lower stress level for the arrestor and particularly for the bridge. The second one is that energy approach does not distinguish natural vibration modes and their influence on stress shape. It should be emphasized that higher vibration modes have a large influence on stress level for rigid structures, for example the bridge. That is the explanation why energy approach gives significantly lower stress level for rigid structures compared with numerical procedure. These two approaches, i.e. the numerical approach and the energy approach support each other.

Table 2. Natural frequencies

Tablica 2. Prirodne frekvencije

Natural frequencies / Prirodne frekvencije, rad/s			
n	arrestor / arestor	bridge / most	bridge and arrestor / most i arestor
1	13,7	0,0	5,6
2	92,9	55,9	45,8
3	270,9	181,1	84,4
4	546,1	377,9	181,1
5	923,5	646,5	251,8

Table 3. Natural periods

Tablica 3. Prirodni periodi

Natural periods / Prirodni periodi, s			
n	arrestor / arestor	bridge / most	bridge and arrestor / most i arestor
1	0,458	/	1,130
2	0,068	0,112	0,137
3	0,023	0,035	0,074
4	0,012	0,017	0,035
5	0,007	0,010	0,025

Appendix a. Study of damping influence on system dynamic response

The influence of damping on bridge and arrestor deformations and stresses is analysed. As mentioned before, damping matrices for bridge and arrestor are derived by taking critical damping for all vibration modes into account. Non-dimensional damping coefficient for calculation is taken to be $\gamma_i = 0{,}03$. Recommended value of this coefficient is between 0,02 and 0,05 for standard vibration analyses. Having in mind that the impact load is present here, i.e. high velocity during the structure deformation, it is necessary to conduct a more detailed analysis of damping influence on structural response. Therefore, the simplified model of bridge and arrestor has been made, Figure A1. The calculation is executed several times with different values of non-dimensional damping coefficient: 0; 0,01; 0,015; 0,02; 0,03 and 0,04. Bridge and arrestor deflections in correlation with different values of non-dimensional damping coefficients are shown in Figures A2 to A7. One can conclude that the damping coefficient does not have significant influence on bridge and arrestor deflection. Damping coefficient influence is significant for bridge stresses, Figures A8 to A13. Time distribution of stress is similar for $\gamma_i = 0{,}0$ and $\gamma_i = 0{,}1$. Large discrepancies can be noticed at $\gamma_i = 0{,}0015$. A further increase of the damping coefficient does not decrease the stress level, i.e. for $\gamma_i = 0{,}02$, $\gamma_i = 0{,}03$ and $\gamma_i = 0{,}04$ the stress level is approximately equal. The bridge stress level is rather influenced by local deformations, i.e. higher vibration modes. At $\gamma_i = 0{,}0$ and $\gamma_i = 0{,}01$ higher modes are still undamped and significantly increase stress levels. Finally, one can conclude that the damping definition described in this chapter has a large influence on higher vibration modes, but its influence on lower modes is negligible.

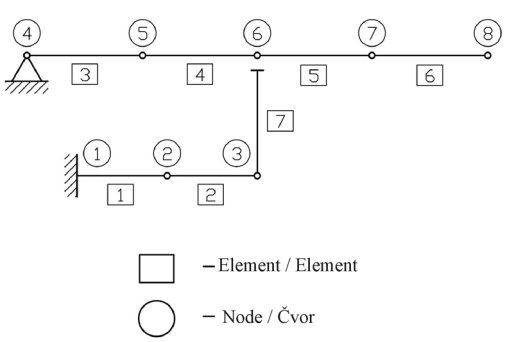

Figure A1. Simplified topology of bridge and arrestor

Figure A1. Pojednostavljena topologija mosta i arestora

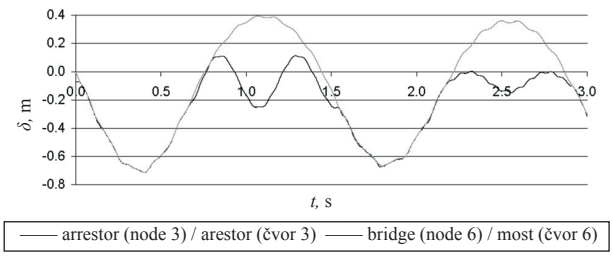

Figure A2. Deflection of arrestor end and bridge contact point, $\gamma_i = 0$

Slika A2. Progib kraja arestora i mjesta kontakta na mostu, $\gamma_i = 0$

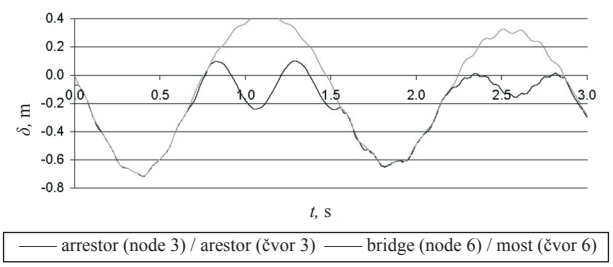

Figure A3. Deflection of arrestor end and bridge contact point, $\gamma_i = 0{,}01$

Slika A3. Progib kraja arestora i mjesta kontakta na mostu, $\gamma_i = 0{,}01$

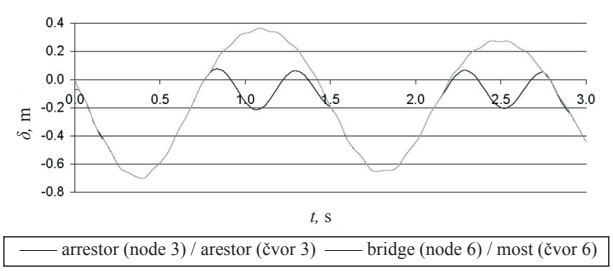

Figure A4. Deflection of arrestor end and bridge contact point, $\gamma_i = 0{,}015$

Slika A4. Progib kraja arestora i mjesta kontakta na mostu, $\gamma_i = 0{,}015$

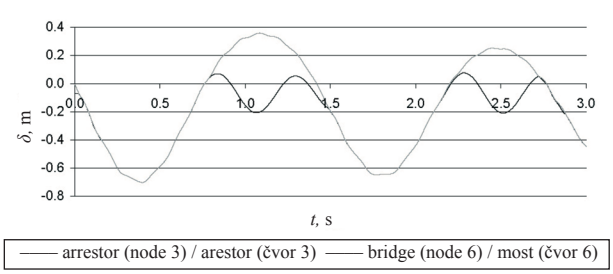

Figure A5. Deflection of arrestor end and bridge contact point, $\gamma_i = 0{,}02$

Slika A5. Progib kraja arestora i mjesta kontakta na mostu, $\gamma_i = 0{,}02$

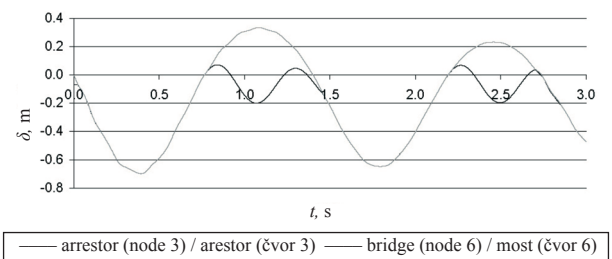

Figure A6. Deflection of arrestor end and bridge contact point, $\gamma_i = 0{,}03$

Slika A6. Progib kraja arestora i mjesta kontakta na mostu, $\gamma_i = 0{,}03$

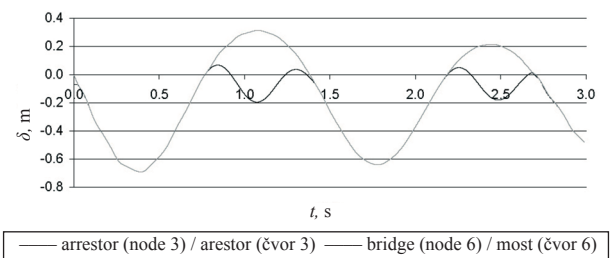

Figure A7. Deflection of arrestor end and bridge contact point, $\gamma_i = 0{,}04$

Slika A7. Progib kraja arestora i mjesta kontakta na mostu, $\gamma_i = 0{,}04$

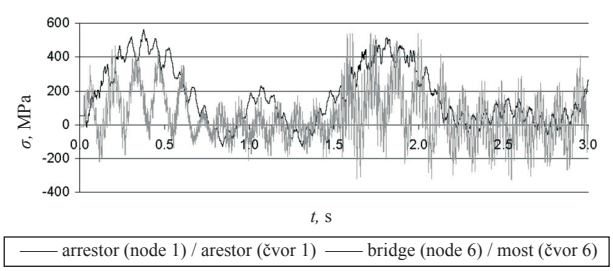

Figure A8. Bending stress at critical cross-section of bridge and arrestor, $\gamma_i = 0{,}0$

Slika A8. Savojno naprezanje u kritičnim presjecima mosta i arestora, $\gamma_i = 0{,}0$

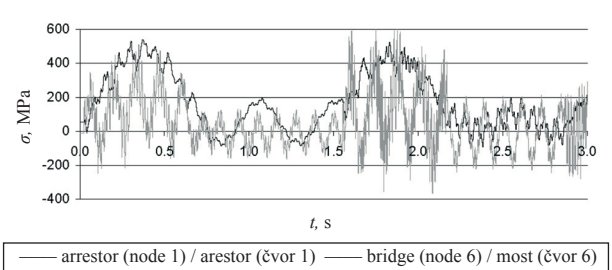

Figure A9. Bending stress at critical cross-section of bridge and arrestor, $\gamma_i = 0{,}01$

Slika A9. Savojno naprezanje u kritičnim presjecima mosta i arestora, $\gamma_i = 0{,}01$

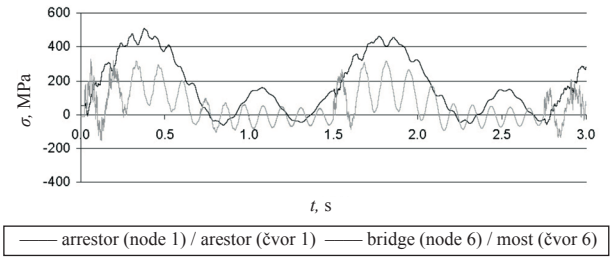

Figure A10. Bending stress at critical cross-section of bridge and arrestor, $\gamma_i = 0{,}015$

Slika A10. Savojno naprezanje u kritičnim presjecima mosta i arestora, $\gamma_i = 0{,}015$

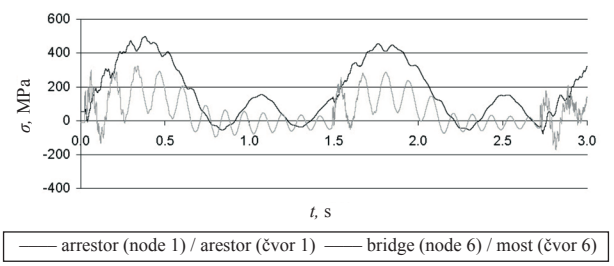

Figure A11. Bending stress at critical cross-section of bridge and arrestor, $\gamma_i = 0{,}02$

Slika A11. Savojno naprezanje u kritičnim presjecima mosta i arestora, $\gamma_i = 0{,}02$

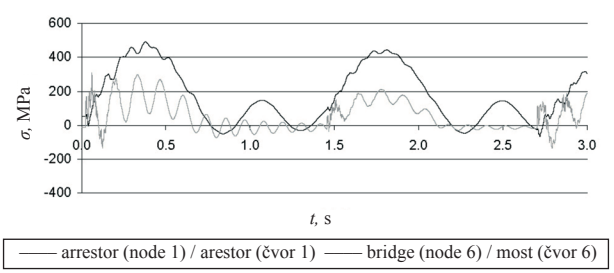

Figure A12. Bending stress at critical cross-section of bridge and arrestor, $\gamma_i = 0{,}03$

Slika A12. Savojno naprezanje u kritičnim presjecima mosta i arestora, $\gamma_i = 0{,}03$

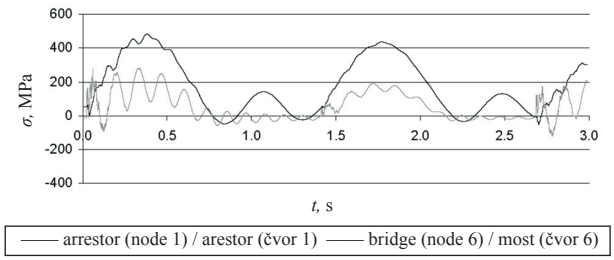

Figure A13. Bending stress at critical cross-section of bridge and arrestor, $\gamma_i = 0{,}04$

Slika A13. Savojno naprezanje u kritičnim presjecima mosta i arestora, $\gamma_i = 0{,}04$

REFERENCES

[1] ALFIREVIĆ, I.: *Strength of materials II*, Technical mechanics library, Book-5, Golden marketing, Zagreb, 2005.

[2] SENJANOVIĆ, I.: *Finite element method in the analysis of ship structures*, University of Zagreb, Zagreb, 1998.

[3] SENJANOVIĆ, I.: *Ship vibrations*, Part 3, Textbook, University of Zagreb, Zagreb, 1981.

[4] Tyne Gangway (Structures) Ltd., Howdon Lane, Wallsend-on-Tyne, England.